

## Structure Function Measurement at HERA

Gregorio Bernardi

LPNHE-Paris, 4 place Jussieu, 75252 Paris Cedex 05, France

## Abstract

Preliminary results<sup>1</sup> on a measurement of the proton structure function  $F_2(x; Q^2)$  are reported for momentum transfers squared  $Q^2$  between  $1.5 \text{ GeV}^2$  and  $5000 \text{ GeV}^2$  and for Bjorken  $x$  between  $5 \cdot 10^{-5}$  and  $0.32$ , using data collected by the HERA experiments H1 and ZEUS in 1994.  $F_2$  increases significantly with decreasing  $x$ , even in the lowest reachable  $Q^2$  region. The data are well described by a Next to Leading Order (NLO) QCD fit, and support within the present precision that the rise at low  $x$  within this  $Q^2$  range is generated "radiatively" via the DGLAP evolution equations. Prospects for future structure function measurements at HERA are briefly mentioned.

## 1 Introduction

The measurement of the inclusive deep inelastic lepton-proton scattering cross section has been of great importance for the understanding of the substructure of the proton [1]. Experiments at HERA extend the previously accessible kinematic range up to very large squared momentum transfers,  $Q^2 > 5 \cdot 10^4 \text{ GeV}^2$ , and to very small values of Bjorken  $x < 10^{-4}$ . The first observations showed a rise of the proton structure function  $F_2(x; Q^2)$  at low  $x < 10^{-2}$  with decreasing  $x$  [2, 3], based on data collected in 1992. This rise was confirmed with the more precise data of 1993 [4, 5]. Such a behaviour is qualitatively expected in the double leading log limit of Quantum Chromodynamics [6]. It is, however, not clarified whether the linear QCD evolution equations, as the conventional DGLAP evolution [7] in  $\ln Q^2$  and/or the BFKL evolution [8] in  $\ln(1/x)$ , describe the rise of  $F_2$  or whether there is a significant effect due to nonlinear parton recombination [9]. Furthermore, it is unclear whether this rise will persist at low  $Q^2$ , say of the order of a few  $\text{GeV}^2$ . For example Regge inspired models expect  $F_2$  to be

<sup>1</sup>Invited talk given at the XXV<sup>th</sup> Workshop on High Energy Physics, Gravitation and Field Theory, held in Protvino, Russia, June 1995. The results presented here are reflecting the status of the measurements reported by the H1 and ZEUS collaboration at the 1995 summer conferences.

after for small  $Q^2$ . The quantitative investigation of the quark-gluon interaction dynamics at low  $x$  is one of the major goals of HERA. It requires high precision for the  $F_2$  measurement and a detailed study of the hadronic final state behaviour [10].

The structure functions  $F_1(x;Q^2)$ ,  $F_2(x;Q^2)$  and  $F_3(x;Q^2)$  are related to the inclusive lepton-photon cross-section

$$\frac{d^2 \sigma_{e^+p}}{dx dQ^2} = \frac{2}{xQ^4} [2xF_1(x;Q^2) + 2(1-y)F_2(x;Q^2) - 2y \frac{y^2}{2} xF_3(x;Q^2)] \quad (1)$$

and depend on the squared four momentum transfer  $Q^2$  and the scaling variable  $x$ . These variables are related to the inelasticity parameter  $y$  and to the total squared centre of mass energy of the collision  $s$  as  $Q^2 = xys$  with  $s = 4E_e E_p$ . However, at low  $Q^2$   $xF_3$  can be neglected and the previous expression can be rewritten as a function of  $F_2$  and  $R$

$$R = \frac{F_2 - 2xF_1}{2xF_1} = \frac{F_L}{2xF_1} \quad (2)$$

$R(x;Q^2)$  could not be measured yet at HERA, but can be computed, supposing that perturbative QCD hold, for a given set of parton densities. Thus  $F_2(x;Q^2)$  can be derived from the double differential cross-section  $d^2\sigma = dx dQ^2$  after experimental and QED radiative corrections. The structure function  $xF_3(x;Q^2)$  has not been measured yet, due to lack of statistics at high  $Q^2$ . However, simple differential cross-section  $d\sigma = dQ^2$  both on neutral currents (exchange of a  $\gamma$  or  $Z^0$ ) or in charged current (exchange of  $W^\pm$ ) have already been published [11, 12]. In the rest of this paper we will consider only the case of the  $\gamma$  exchange.

In 1994 the incident electron energy was  $E_e = 27.5$  GeV and the proton energy was  $E_p = 820$  GeV. The data were recorded with the H1 [13] and ZEUS [14] detectors. A salient feature of the HERA collider experiments is the possibility of measuring not only the scattered electron but also the complete hadronic final state, apart from losses near the beam pipe. This means that the kinematic variables  $x$ ;  $y$  and  $Q^2$  can be determined with complementary methods which experimentally are sensitive to different systematic effects. The comparison of the results obtained with different methods improves the accuracy of the  $F_2$  measurement. A convenient combination of the results ensures maximum coverage of the available kinematic range.

In this paper after a description of the data samples (section 2) and of the kinematic reconstruction/event selection used (section 3) we provide the  $F_2$  measurement in section 4, and its interpretation at low  $Q^2$  and in terms of perturbative QCD in section 5, before giving some prospects in conclusion.

## 2 Data Samples

In 1994 both experiments have reduced the minimum  $Q^2$  at which they could measure  $F_2$  using several techniques. For DIS events at low  $Q^2$  the electron is scattered under a

large angle  $\theta_e$  (the polar angles are defined w.r.t the proton beam direction, termed "forward" region). Therefore the acceptance of electrons in the backward region has to be increased or the incident electron energy to be reduced to go down in  $Q^2$ . This was realized as follows.

i) both experiments were able to diminish the region around the backward beam pipe in which the electron could not be measured reliably in 93, thus increasing the maximum polar angle of the scattered electron (cf [15, 16] for details). This large statistic sample, taken with the nominal HERA conditions is called the "nominal vertex" sample. Its integrated luminosity is between 2 and 3 pb<sup>-1</sup>, depending on the analysis/experiment.

ii) Following a pilot exercise performed last year, 58 nb<sup>-1</sup> of data was collected for which the interaction point was shifted by + 62 cm, in the forward direction, resulting in an increase of the electron acceptance. This sample is referred to as the "shifted vertex" data sample. In H1 the low  $Q^2$  region was also covered by analyzing events which originated from the "early" proton satellite bunch, present during all periods of the HERA operation, which collided with an electron bunch at a position shifted by + 63 cm. These data, referred to as the "satellite" data sample amount to ' 3% of the total data and correspond to a total "luminosity" of 68 nb<sup>-1</sup>.

iii) Both experiments used DIS events which underwent initial state photon radiation detected in an appropriate photon tagger to measure  $F_2$  at lower  $Q^2$  (so called "radiative" sample [17]). The incident electron energy which participate in the hard scattering is thus reduced, and so is the  $Q^2$ .

The luminosity was determined from the measured cross section of the Bethe Heitler reaction  $e p \rightarrow e p \gamma$ , measuring the hard photon bremsstrahlung data only. The precision of the luminosity for the nominal vertex position data amounts to 1.5%, i.e. an improvement of a factor 3 w.r.t the analysis of the 1993 data. For the shifted vertex data the luminosity uncertainty is higher (4.5% for H1). The luminosity of the satellite data sample was obtained from the measured luminosity for the shifted vertex data multiplied by the efficiency corrected event ratio in a kinematic region common to both data sets. The uncertainty of that luminosity determination was estimated to be 5%.

### 3 Kinematics and Event Selection

The kinematic variables of the inclusive scattering process  $e p \rightarrow e X$  can be reconstructed in different ways using measured quantities from the hadronic final state and from the scattered electron. The choice of the reconstruction method for  $Q^2$  and  $y$  determines the size of systematic errors, acceptance and radiative corrections. The

basic formulae for  $Q^2$  and  $y$  used in the different methods are summarized below,  $x$  being obtained from  $Q^2 = xys$ . For the electron method

$$y_e = 1 - \frac{E_e^0}{E_e} \sin^2 \frac{\theta_e}{2} \quad Q_e^2 = \frac{E_e^0 \sin^2 \frac{\theta_e}{2}}{1 - y_e} \quad (3)$$

The resolution in  $Q_e^2$  is 4% while the  $y_e$  measurement degrades as  $1/y_e$  and cannot be used for  $y_e < 0.05$ . In the low  $y$  region it is, however, possible to use the hadronic methods for which it is convenient to define the following variables

$$y_h = \frac{\sum_h E_h}{E_e} \quad p_{T,h}^2 = \left( \sum_h p_{x,h} \right)^2 + \left( \sum_h p_{y,h} \right)^2 \quad (4)$$

Here  $E; p_x; p_y; p_z$  are the four-momentum vector components of each particle and the summation is over all hadronic final state particles. The standard definitions for  $y_h$  and  $p_{T,h}$  are

$$y_h = \frac{p_{T,h}}{2E_e} \quad \tan \frac{\theta_h}{2} = \frac{p_{T,h}}{p_{z,h}} \quad (5)$$

The combination of  $y_h$  and  $Q_e^2$  defines the fixed method which is well suited for medium and low  $y$  measurements. The same is true for the double-angle method which makes use only of  $\theta_e$  and  $\theta_h$  and is thus insensitive to the absolute energy calibration:

$$y_{DA} = \frac{\tan \frac{\theta_h}{2}}{\tan \frac{\theta_e}{2} + \tan \frac{\theta_h}{2}} \quad Q_{DA}^2 = 4E_e^2 \frac{\cot \frac{\theta_e}{2}}{\tan \frac{\theta_e}{2} + \tan \frac{\theta_h}{2}} \quad (6)$$

The formulae for the  $\gamma$  method are constructed requiring  $Q^2$  and  $y$  to be independent of the incident electron energy. Using the conservation of the total  $E - P_z$   $\sum_i E_i - p_{z,i}$ , the sum extending over all particles of the event,  $2E_e$  is replaced by  $\sum_i E_i - p_{z,i} + E_e^0(1 - \cos \theta_e)$  which gives

$$y = \frac{p_{T,h}^2}{\sum_i E_i - p_{z,i} + E_e^0(1 - \cos \theta_e)} \quad Q^2 = \frac{E_e^0 \sin^2 \frac{\theta_e}{2}}{1 - y} \quad (7)$$

By construction  $y$  and  $Q^2$  are independent of initial state photon radiation. With respect to  $y_h$  the modified quantity  $y$  is less sensitive to the hadronic measurement at high  $y$ , since the  $\gamma$  term dominates the total  $E - P_z$  of the event. At low  $y$ ,  $y_h$  and  $y$  are equivalent.

H1 measures  $F_2$  with the electron and the  $\gamma$  method and after a complete consistency check uses the electron method for  $y > 0.15$  and the  $\gamma$  method for  $y < 0.15$ . ZEUS measures  $F_2$  with the electron and the double angle method and for the final results uses the electron method at low  $Q^2$  and the double angle method for high  $Q^2$  ( $Q^2 > 15 \text{ GeV}^2$ ). The binning in  $x$  and  $Q^2$  was chosen to match the resolution in these variables. It was set at 5 (8) bins per order in magnitude in  $x$  ( $Q^2$ ) for the H1

experiment and about twice as coarse for the ZEUS experiment in  $x$  (similar to H1 in  $Q^2$ ).

The event selection is similar in the two experiments. Events are filtered on-line using calorimetric triggers which requests an electromagnetic cluster of at least 5 GeV not vetoed by a trigger element signing a beam background event. Online, further electron identification criteria are applied (track-cluster link, shower shape and radius) and a minimum energy of 8 (11) GeV is requested in ZEUS (H1). H1 requests a reconstructed vertex within 3 of the expected interaction position, while ZEUS requires that the quantity  $\sqrt{E_e^2 - p_e^2} \cos \theta_e$  satisfies  $35 \text{ GeV} < \sqrt{E_e^2 - p_e^2} \cos \theta_e < 65 \text{ GeV}$ . If no particle escapes detection,  $\sqrt{E_e^2 - p_e^2} \cos \theta_e = 2E = 55 \text{ GeV}$ , so the cut reduces the photoproduction background and the size of the radiative corrections. The only significant background left after the selection comes from photoproduction in which a hadronic shower fakes an electron. In H1 for instance, it has been estimated consistently both from the data and from Monte Carlo simulation and amounts to less than 3% except in a few bins where it can reach values up to 15%. It is subtracted statistically bin by bin and an error of 30% is assigned to it.

The acceptance and the response of the detector has been studied and understood in great detail by the two experiments: More than two millions Monte Carlo DIS events were generated using DJANGO [18] and different quark distribution parametrizations, corresponding to an integrated luminosity of approximately  $20 \text{ pb}^{-1}$ . The program is based on HERACLES [19] for the electroweak interaction and on LEPTO [20] to simulate the hadronic final state. HERACLES includes first order radiative corrections, the simulation of real bremsstrahlung photons and the longitudinal structure function. The acceptance corrections were performed using the GRV [34] or the MRS parametrization [21], which both describe rather well the HERA  $F_2$  results of 1993 for  $Q^2 > 10 \text{ GeV}^2$ . LEPTO uses the colour dipole model (CDM) as implemented in ARIADNE [22] which is in good agreement with data on the energy flow and other characteristics of the final state as measured by H1 [23] and ZEUS [24]. For the estimation of systematic errors connected with the topology of the hadronic final state, the HERWIG model [25] was used in a dedicated analysis. Based on the GEANT program [26] the detector response was simulated in detail. After this step the Monte Carlo events were subject to the same reconstruction and analysis chain as the real data.

## 4 Structure Function Measurement

The structure function  $F_2(x; Q^2)$  was derived after radiative corrections from the one-photon exchange cross section

$$\frac{d^2}{dx dQ^2} = \frac{2}{Q^4 x} \left( 2 - 2y + \frac{y^2}{1+R} \right) F_2(x; Q^2) \quad (8)$$

Effects due to Z boson exchange are smaller than 2%. The structure function ratio  $R = F_2 = 2xF_1 - 1$  has not been measured yet at HERA and was calculated using the QCD relation [27] and the GRV structure function parametrization. Compared to the 1993 data analyses [4, 5] the  $F_2$  measurement has been extended to lower  $Q^2$  (from  $4.5 \text{ GeV}^2$  to  $1.5 \text{ GeV}^2$ ), and to lower and higher  $x$  (from  $1.8 \cdot 10^{-4}$  to  $0.13$  to  $5 \cdot 10^{-5}$  to  $0.32$ ). The determination of the structure function requires the measured event numbers to be converted to the bin averaged cross section based on the Monte Carlo acceptance calculation. All detector efficiencies were determined from the data using the redundancy of the apparatus. Apart from very small extra corrections all efficiencies are correctly reproduced by the Monte Carlo simulation. The bin averaged cross section was corrected for higher order QED radiative contributions and a bin size correction was performed. This determined the one-photon exchange cross section which according to eq.8 led to the values for  $F_2(x; Q^2)$ .

Due to the different data sets available: "nominal vertex" data, "radiative events", "shifted vertex" data and "satellite" data, which have different acceptances and use for a given  $Q^2; x$  point different parts of the detectors, cross checks could be made in kinematic regions of overlap. The results were found to be in very good agreement with each other for all kinematic reconstruction methods used.

The large available statistics allows to make very detailed studies on the detector response: efficiencies and calibration. As a result the systematic errors on many effects are reduced, compared to the 1993 data analysis. Here only a brief summary of these preliminary errors is given, referring the reader to the original and forthcoming  $F_2$  publications: For the electron method the main source of error are the energy calibration (known at 1.5% level in 1994), the knowledge of the electron identification efficiency and to a lesser extent the error on the polar angle of the scattered electron, ( $\theta = 1 \text{ m rad}$ ) in particular at the lowest  $Q^2$  and the radiative corrections at low  $x$ . For the  $\mu$  method, the knowledge of the absolute energy scale for the hadrons, the fraction of hadrons which stay undetected in particular at low  $x$ , due to calorimetric thresholds and to a lesser extent the electron energy calibration are the dominating factors. For the double angle method, the major problem comes from the precision in the resolution of the hadronic angle at low  $x$  and low  $Q^2$ . Further uncertainties common to all methods (selection, structure function dependance etc.) were also studied. The preliminary error on the 1994 data ranges between 10 and 20% with expected final values for publication below 10%.

The preliminary results of H1 and ZEUS are shown in fig.1, in bins of fixed  $Q^2$ . The rise of  $F_2$  at low  $x$  is confirmed with the higher precision, and is now observed down to the lowest  $Q^2$  measured ( $1.5 \text{ GeV}^2$ ). The observed good agreement between H1 and ZEUS and the smooth transition between the HERA and the fixed target (E665, NMC) data consolidates this result which can thus be confronted to theoretical expectations. The steepness of the low  $x$  rise increases visibly with the  $Q^2$ , a characteristic expected from perturbative QCD. This rise cannot be attributed to the presence of "diffractive"

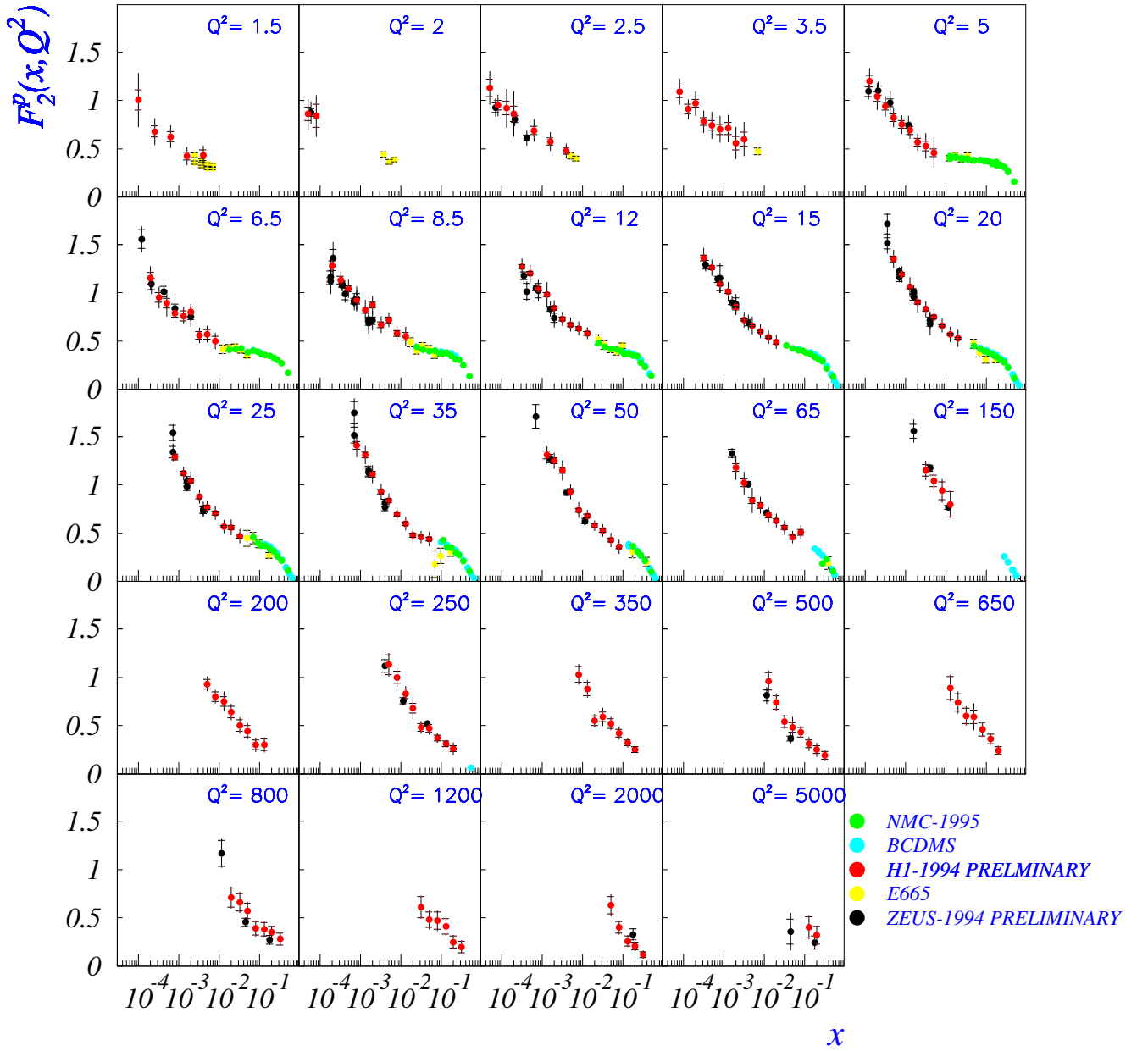


Figure 1: Preliminary measurement of the proton structure function  $F_2(x; Q^2)$  as function of  $x$  in different bins of  $Q^2$ . The inner error bar is the statistical error. The full error represents the statistical and systematic errors added in quadrature.

events in the DIS sample since their proportion has been shown to stay essentially constant ( 10% ) independently of  $x$  and  $Q^2$  [28, 29].

## 5 Low $Q^2$ and Perturbative QCD

A test of perturbative QCD is displayed in fig. 2 which represents the results of Next to Leading Order (NLO) QCD fit performed by H1 as explained in [30] on the data with  $Q^2 \leq 5 \text{ GeV}^2$ . In order to constrain the structure function  $F_2$  at high  $x$ , data from the fixed target scattering experiment NMC [31] and BCDMS [32] are used, avoiding regions where higher twist and target mass effects could become important.

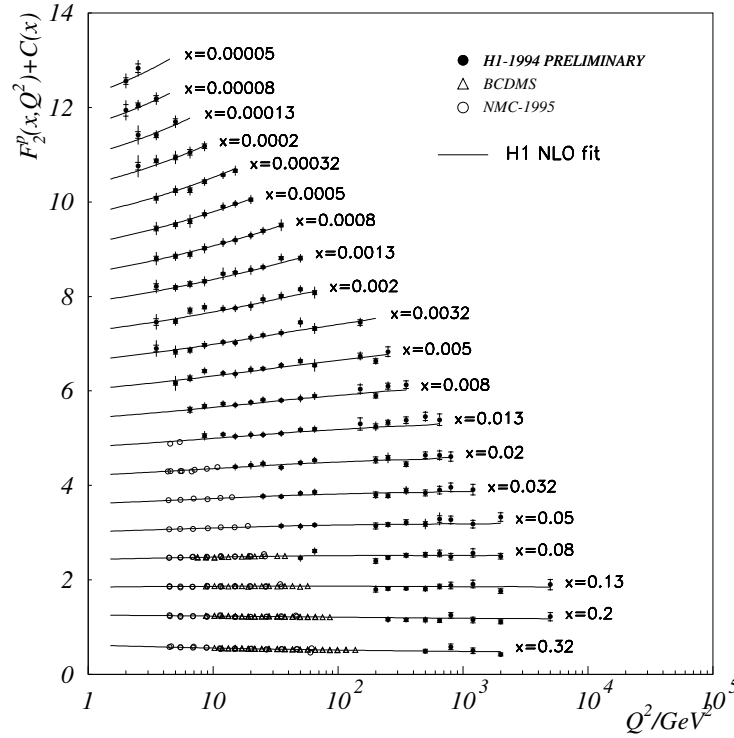


Figure 2: Preliminary measurement of  $F_2(x; Q^2)$ . The H1 data is consistent with the fixed target experiments BCDMS and NMC. The curve represents the NLO QCD fit described in the text. The gap visible around  $100 \text{ GeV}^2$  corresponds to a boundary region between two calorimeters in the H1 detector, which is not completely analyzed yet.

The  $F_2$  behaviour can be well described by the DGLAP evolution equations within the present preliminary errors. The data for  $Q^2$  values below  $5 \text{ GeV}^2$  are also compatible with the extrapolation of the fit in this region, as can be seen in the figure.



This preliminary result is consistent with the published QCD analysis of H1 and ZEUS 1993 data, which allowed to determine the gluon density in the proton, and observe its steep rise at low  $x$  as displayed in Fig. 3 for  $Q^2 = 20 \text{ GeV}^2$ .

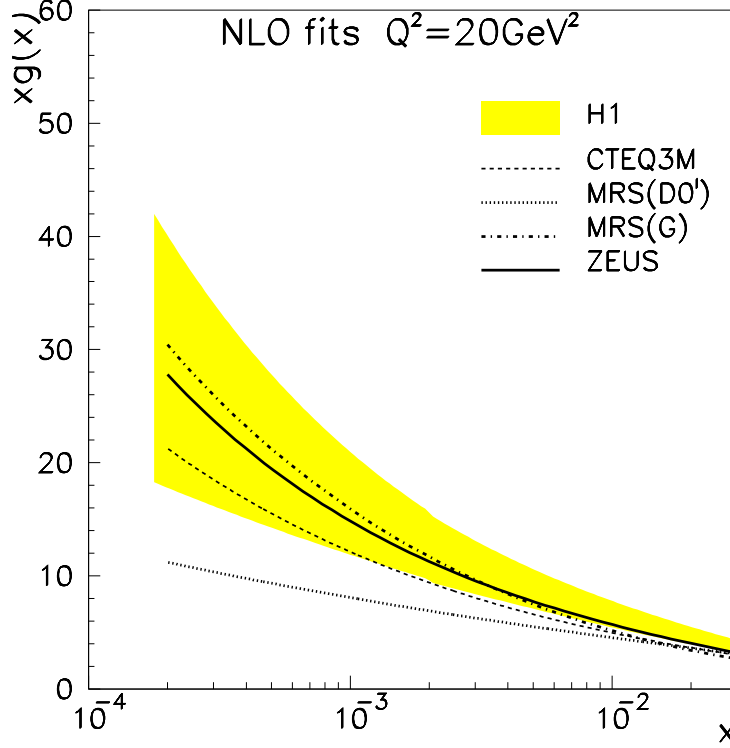


Figure 3: Preliminary measurement of the gluon density from NLO QCD fit. The H1 result is shown with the complete systematic error band, for ZEUS only the value of the gluon density is shown, the error band is similar to the H1 one.

Another test of perturbative QCD lies in observing the asymptotic behaviour as suggested by early studies [6]. Ball and Forte [33] have recently shown that evolving a flat input distribution at some  $Q_0$ , of the order of  $1 \text{ GeV}^2$ , with the DGLAP equations leads to a strong rise of  $F_2$  at low  $x$  in the region measured by HERA. An interesting feature is that if QCD evolution is the underlying dynamics of the rise, perturbative QCD predicts that at large  $Q^2$  and small  $x$  the structure function exhibits double scaling in the two variables defined as:

$$\eta = \frac{\log(x_0/x)}{\log(t/t_0)}; \quad \frac{\log(x_0/x)}{\log(t/t_0)} = \frac{\log(x_0/x)}{\log(t/t_0)} \quad \text{with } t = \log(Q^2/Q_0^2) \quad (9)$$

In Figure 4 the H1 data are presented in the variables  $\eta$  and  $\tau$ , taking the boundary conditions to be  $x_0 = 0.1$  and  $Q_0^2 = 0.5 \text{ GeV}^2$ , and  $\tau_0 = 185 \text{ MeV}$ . In a previous

analysis [30] the value  $Q_0^2 = 1 \text{ GeV}^2$  was chosen, but the new low  $Q^2$  data seems to indicate that  $F_2$  is not yet flat for this  $Q^2$  value. The measured values of  $F_2$  are rescaled by

$$R_F^0(\rho; Q^2) = 8.1 \exp\left(-\frac{1}{2} \log(\rho) + \log(-)\right); \quad (10)$$

to remove the part of the leading subasymptotic behaviour which can be calculated in a model independent way;  $\log(R_F^0 F_2)$  is then predicted to rise linearly with  $\sigma$ . Scaling in  $\rho$  can be shown by multiplying  $F_2$  by the factor  $R_F = R_F^0 e^{Q^2/2}$ . Here  $2/3 = b_0$  with  $b_0$  being the leading order coefficient of the  $\beta$  function of the QCD renormalization group equation for four flavours,  $\beta = 1/36$  for four flavours and three colours.

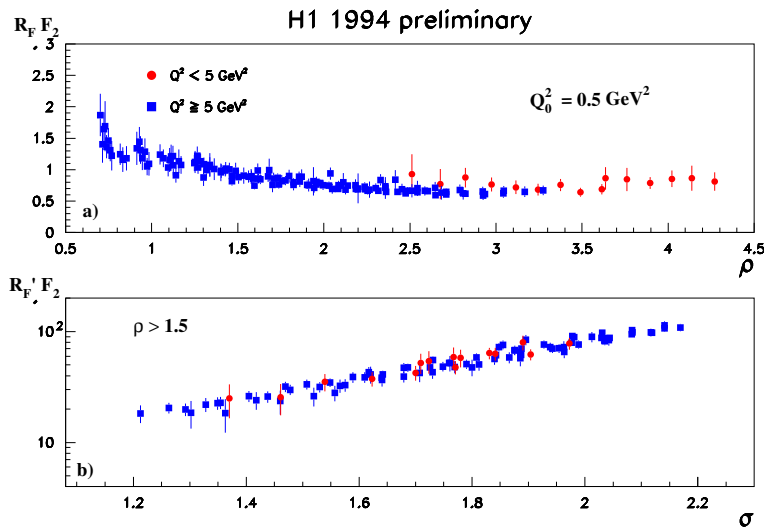


Figure 4: The rescaled structure functions  $R_F F_2$  and  $R_F^0 F_2$  (preliminary) plotted versus the variables  $\rho$  and  $\sigma$  defined in the text. Only data with  $\rho > 1.5$  are shown in b.

Fig. 4a shows  $R_F F_2$  versus  $\rho$ . Scaling roughly sets in for  $\rho > 1.5$ . Fig. 4b, for  $\rho > 1.5$ , shows scaling behaviour, namely a linear of  $\log(R_F^0 F_2)$  with  $\sigma$ .

These observations suggest that perturbative QCD could be already valid at  $Q^2 = 1$  or  $2 \text{ GeV}^2$ . Indeed within the present precision we can observe in fig. 5 the validity of the Glück, Reya, Vogt (GRV) model [34] which assumes that all low  $x$  partons are generated "radiatively" starting from a very low initial  $Q^2 = 0.34 \text{ GeV}^2$  scale, in which both gluon and quark densities are "valence" like. This result appears surprising since perturbative QCD does not apply at such a low scale, but the HERA results and the E665 [35] preliminary results follow the GRV expectations as early as  $0.8 \text{ GeV}^2$ . More precise data are needed to further constrain the model and draw definite conclusions on the dynamics underlying the low  $x$  rise. Nevertheless these results appear

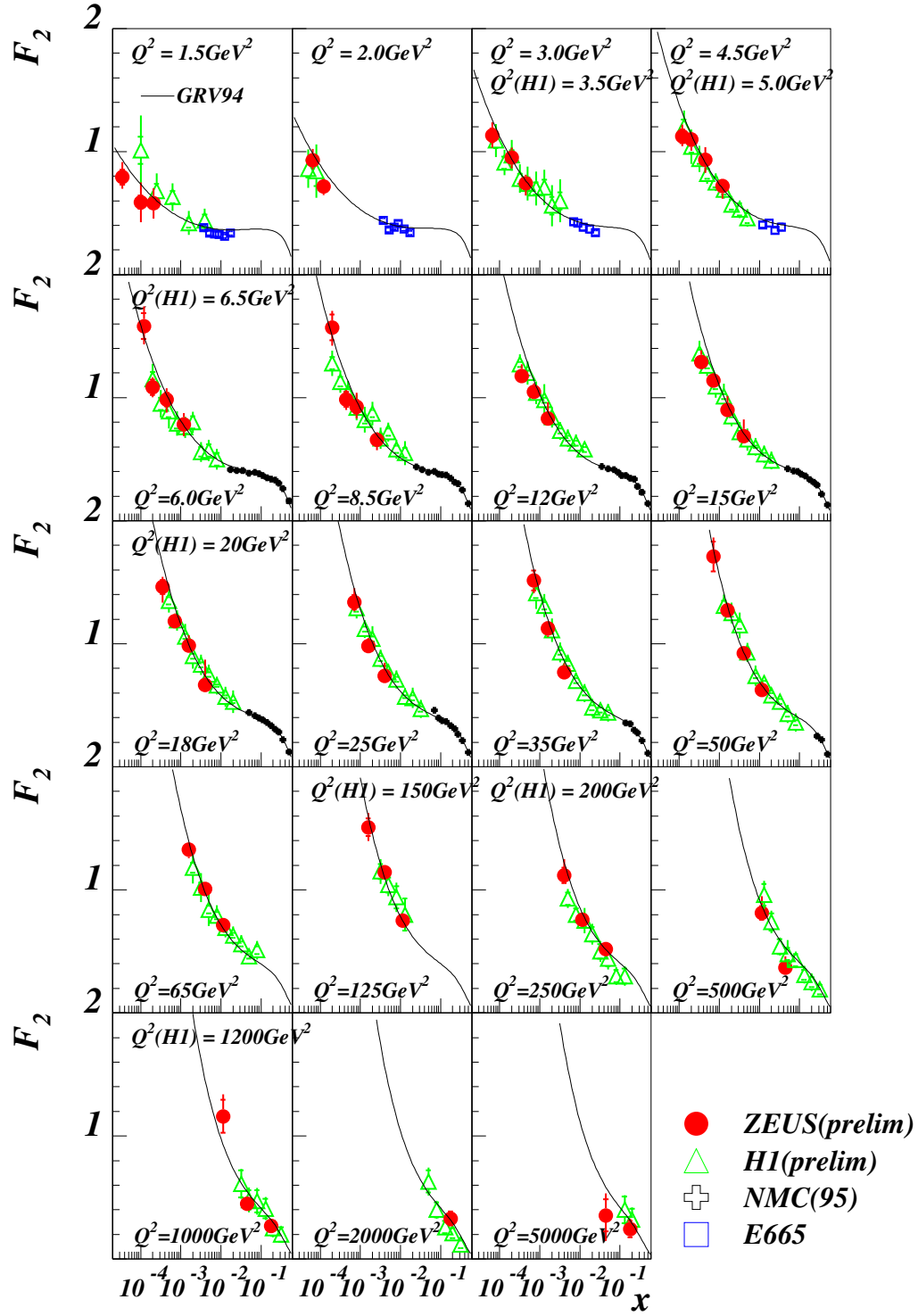


Figure 5: Preliminary measurement of the proton structure function  $F_2(x; Q^2)$  by H1 and ZEUS, compared to the results of the E665 and NMC experiments and to the prediction of the GRV model [34] over the full  $Q^2$  range.

already very promising for the DGLAP evolution equations which might not need to be supplemented by the BFKL evolution at low  $x$ , in the HERA kinematic domain.

Focusing now on low  $Q^2$ , the persistent rise of  $F_2$  at low  $x$ , when going down in  $Q^2$  indicates that the photoproduction regime has not been reached yet. This can be seen in Fig. 6 which displays the behaviour of the total cross-section of the proton-virtual photon system as a function of  $W$ , the invariant mass of the  $\gamma p$  system (at low  $x$ ,  $W \approx \sqrt{Q^2 + x}$ ).  $F_2$  is related to the total cross-section of the proton-virtual photon interaction ( $\sigma_{\text{tot}}(\gamma^* p)$ ) via

$$\sigma_{\text{tot}}(\gamma^* p) = \frac{4}{Q^2} F_2(W; Q^2). \quad (11)$$

The  $\sigma_{\text{tot}}$  growth can be contrasted with the weak rise with  $W$  of the total real photo-production cross-section in the same range of  $W$ : 20–250 GeV [36, 37]

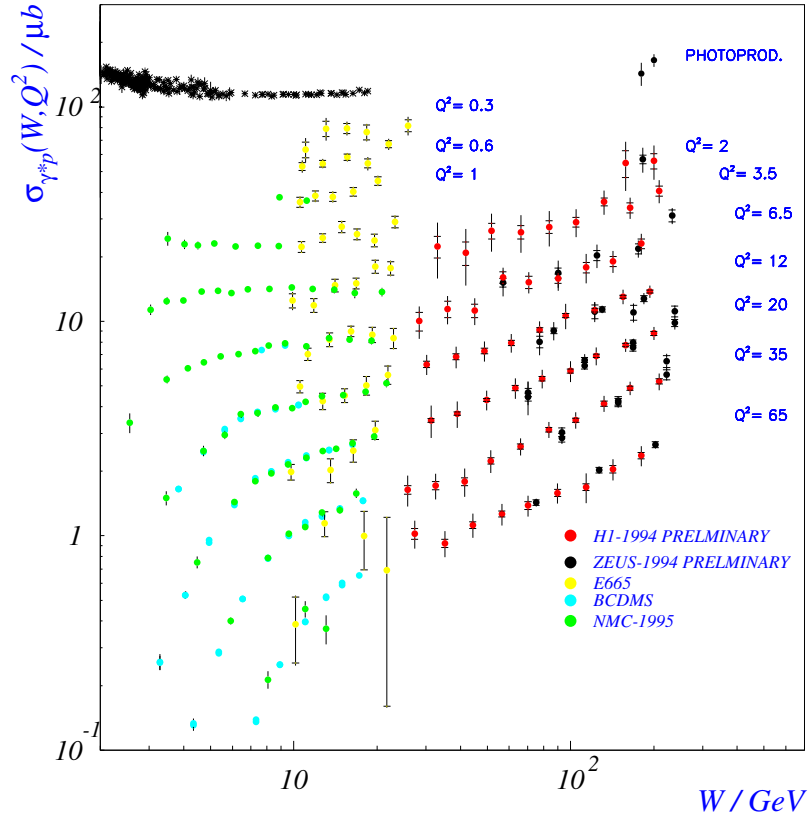


Figure 6: Preliminary measurement of the cross-section  $\sigma_{\text{tot}}(\gamma^* p)$  as a function of  $W$  and  $Q^2$ . Results from DIS are compared with the measurements in photoproduction. For the readability of the plot, not all  $Q^2$  bins are shown.

The Regge inspired models DOLA [38] and CKMT [39] which can describe the behaviour of  $F_2(p)$  predicts a rather flat behaviour of  $F_2$  at a few  $\text{GeV}^2$ . As shown in fig. 7, the DOLA model clearly fails before  $1.5 \text{ GeV}^2$ , while the CKMT model which assumes that the "bare" pomeron visible at high  $Q^2$  has a higher trajectory intercept (0.24) than the "effective" pomeron involved in "soft" interactions (0.08) undershoots the data in a less critical manner. In this same plot we can also notice the similarity above  $5 \text{ GeV}^2$  between the different parametrizations (GRV, MRS, CTEQ [34, 41, 40]) which use essentially the same data to determine their parton distributions at the reference scale.

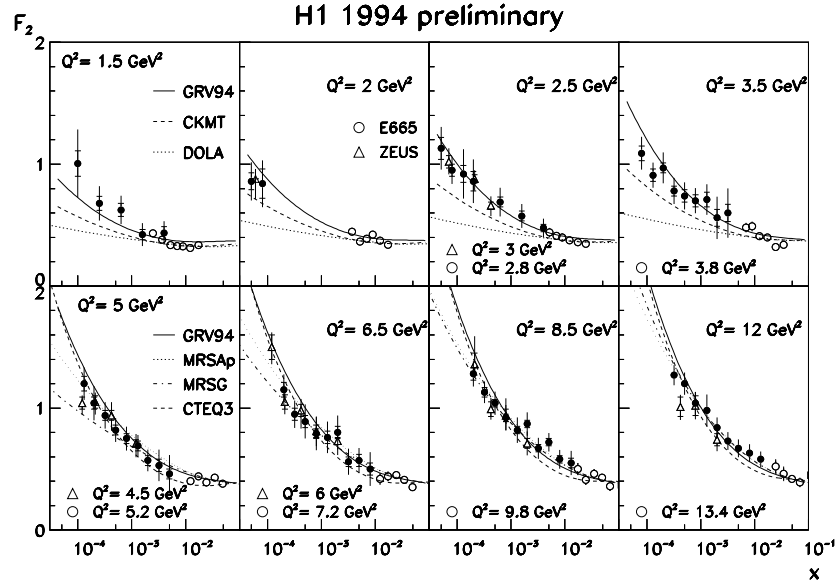


Figure 7: Preliminary measurement of the proton structure function  $F_2(x; Q^2)$  in the low  $Q^2$  region by H1 and ZEUS, together with results from the E665 experiment. Different predictions for  $F_2$  are compared to the data. The DOLA and CKMT curves are only shown for the upper row of  $Q^2$  bins; CTEQ 3M, MRSg and MRSa' are shown for the lower row; GRV is shown for the full range.

## 6 Prospects for Structure function measurements at HERA

The HERA structure function program is still in its infancy, but has already provided exciting results at low  $x$ . The dynamics underlying the behaviour of the structure function can be studied in an exclusive way using jets or particle spectra, since HERA is a collider equipped with (two) 4 detectors. In the next 2 or 3 years  $F_L$  will be

measured, by taking data at different beam energies in order to keep  $x$  and  $Q^2$  constant while varying  $y$ , thus improving the knowledge on  $F_2$  and on QCD. The statistics will increase in such a way that a first measurement of  $xF_3$  will be made, and a precise determination of  $\alpha_s$  should be possible. In 95, both experiments have upgraded their detector in the backward area in order to reach lower  $Q^2$  ( $\sim 0.1 \text{ GeV}^2$ ) with good precision. This year will thus be devoted to understand the questions raised in this paper concerning the low  $x$  and low  $Q^2$  dynamics and to open up further stringent test of QCD, in particular about the behaviour of the high parton density.

#### Acknowledgements

I would like to thank the organizers and in particular Vladimir Petrov to have made such a nice workshop in the quiet town of Protvino, and to have invited me to discover Russia for the first time. I would also like to thank my close collaborators, Ursula Bassler, Beatriz Gonzalez-Pineiro, all the friends of the H1 structure function group and the ZEUS collaboration with whom we obtained the results described above. Special thanks go to Ursula for her help in the finalization of this paper.

## References

- [1] for a recent review see: J. Feltesse, DAPNIA-SPP-94-35 (1994), Invited talk at the 27. International Conference on High Energy Physics, Glasgow, Scotland, 1994.
- [2] H1 Collab., I. Abt et al., Nucl. Phys. B 407 (1993) 515.
- [3] ZEUS Collab., M. Derrick et al., Phys. Lett. B 316 (1993) 412.
- [4] H1 Collab., T. Ahmed et al., Nucl. Phys. B 439 (1995) 471.
- [5] ZEUS Collab., M. Derrick et al., Z. Phys. C 65 (1995), 379.
- [6] A. De Rújula et al., Phys. Rev. D 10 (1974) 1649.
- [7] Yu. L. Dokshitzer, Sov. Phys. JETP 46 (1977) 641;  
V. N. Gribov and L. N. Lipatov, Sov. J. Nucl. Phys. 15 (1972) 438 and 675;  
G. Altarelli and G. Parisi, Nucl. Phys. B 126 (1977) 297.
- [8] E. A. Kuraev, L. N. Lipatov and V. S. Fadin, Sov. Phys. JETP 45 (1977) 19; 9;  
Y. Y. Balitsky and L. N. Lipatov, Sov. J. Nucl. Phys. 28 (1978) 822.
- [9] L. V. Gribov, E. M. Levin and M. G. Ryskin, Phys. Rep. 100 (1983) 1;  
A. H. Mueller and N. Quir, Nucl. Phys. B 268 (1986) 427.

- [10] H1 Collab, S. Aid et al, DESY preprint 95-108 (1995).
- [11] H1 Collab, S. Aid et al, DESY preprint 95-102 (1995).
- [12] ZEUS Collab, M. Derrick et al, Phys. Rev. Lett. 75 (1995) 1006.
- [13] H1 Collab., I. Abt et al, DESY 93-103 (1993).
- [14] ZEUS Collab., M. Derrick et al, Phys. Lett. B 293 (1992) 465.
- [15] H1 Collab., contributed paper to 1995 EPS conference, Brussels, EPS-470 (1995).
- [16] ZEUS Collab., contributed paper to 1995 EPS conference, Brussels, EPS-392 (1995).
- [17] H1 Collab., contributed paper to 1995 EPS conference, Brussels, EPS-472 (1995).
- [18] G. A. Schuler and H. Spiesberger, Proceedings of the Workshop Physics at HERA, vol. 3, eds. W. Buchmüller, G. Ingelman, DESY (1992) 1419.
- [19] A. Kwiatkowski, H. Spiesberger and H.-J. Mohring, Computer Phys. Comm. 69 (1992) 155.
- [20] G. Ingelman, Proceedings of the Workshop Physics at HERA, vol. 3, eds. W. Buchmüller, G. Ingelman, DESY (1992) 1366.
- [21] A. D. Martin, W. J. Stirling and R. G. Roberts, Proceedings of the Workshop on Quantum Field Theory Theoretical Aspects of High Energy Physics, eds. B. Geyer and E. M. Ilgenfritz (1993) 11.
- [22] L. Lonnblad, Computer Phys. Comm. 71 (1992) 15.
- [23] H1 Collab., I. Abt et al, Z. Phys. C 63 (1994) 377.
- [24] ZEUS Collab., M. Derrick et al, Z. Phys. C 59 (1993), 231.
- [25] G. Marchesini et al, Computer Phys. Comm. 67 (1992) 465.
- [26] R. Brun et al, GEANT 3 User's Guide, CERN DD/EE 84(1), Geneva (1987).
- [27] G. Altarelli and G. Martinelli, Phys. Lett. B 76 (1978) 89.
- [28] H1 Collab., contributed paper to 1995 EPS conference, Brussels, EPS-0491 (1995).
- [29] ZEUS Collab., contributed paper to 1995 EPS conference, Brussels, EPS-0393 (1995).
- [30] H1 Collab., S. Aid et al, Phys. Lett. B 354 494 (1995).

- [31] NM C Collab., P. Amaudruz et al, Phys. Lett. B 259 (1992) 159.
- [32] BCDMS Collab., A.C. Benvenuti et al, Phys. Lett. B 237 (1990) 592.
- [33] R.D. Ball, S. Forte, Phys. Lett. B 335 (1994) 77.
- [34] M. Glück, E. Reya and A. Vogt, Z. Phys. C 67 (1995) 433.
- [35] E665 Collab., M.R. Adams et al, Phys. Rev. Lett. 75 (1995) 1466.
- [36] H1 Collab., S. Aid et al, DESY 95-162 (1995).
- [37] ZEUS Collab., M. Derrick et al, Z. Phys. C 63 (1994) 391.
- [38] A. Donnachie and P.V. Landshof, Z. Phys. C 61 (1994) 139.
- [39] A. Capella et al, Phys. Lett. B 337 (1994) 358.
- [40] CTEQ Collab., J. Botts et al, Phys. Lett. 304B (1993) 15;  
CTEQ Collab., J. Botts et al. (to be published).
- [41] A.D. Martin, W.J. Stirling and R.G. Roberts, RAL preprint RAL-95-021 (1995).